First Wide-Area Dutch Peatland Subsidence Estimates Based on InSAR

Conroy, Philip; Lumban-Gaol, Yustisi; Van Diepen, Simon; Van Leijen, Freek; Hanssen, Ramon F.

DOI
10.1109/IGARSS53475.2024.10642504

Publication date
2024

Document Version
Final published version

Citation (APA)
Conroy, P., Lumban-Gaol, Y., Van Diepen, S., Van Leijen, F., & Hanssen, R. F. (2024). *First Wide-Area Dutch Peatland Subsidence Estimates Based on InSAR*. 10732-10735. Paper presented at 2024 IEEE International Geoscience and Remote Sensing Symposium, IGARSS 2024, Athens, Greece. https://doi.org/10.1109/IGARSS53475.2024.10642504

IGARSS 2024 - 2024 IEEE International Geoscience and Remote Sensing Symposium | 979-8-3503-6032-5/24/$31.00 ©2024 IEEE | DOI: 10.1109/IGARSS53475.2024.10642504

FIRST WIDE-AREA DUTCH PEATLAND SUBSIDENCE ESTIMATES BASED ON INSAR

Philip Conroy, Yustisi Lumban-Gaol, Simon van Diepen, Freek van Leijen, Ramon F. Hanssen

Department of Geoscience and Remote Sensing, Delft University of Technology
Stevinweg 1, 2628 CN Delft, The Netherlands

ABSTRACT

We present the preliminary results of an InSAR analysis of peatland surface motion covering a large spatial and temporal extent. This work is the first large scale analysis of the Dutch Green Heart region, and is made possible using a novel distributed scatter (DS) InSAR processing method. This method is designed to handle breakages in the observed interferometric phase time series which occur due to temporal decorrelation, which we designate with the term loss-of-lock.

1. INTRODUCTION

Northern peatlands are critically important regions for carbon emissions, water security and biodiversity. However, their behaviour and interactions with the underlying water system remain poorly understood due to the difficulties in producing observations with sufficient quality and spatiotemporal resolution. While InSAR is a viable alternative to costly and localized in-situ measurements, the technique often suffers from drastic losses of coherence in the spring and summer months when producing time-series observations of peatlands. This significantly limits the effectiveness of InSAR as a tool to monitor peatland surface dynamics [1, 2, 3, 4].

The seasonal loss of coherence experienced in this peatland region results in a phenomenon we call *loss-of-lock*, which is a breakage of the InSAR time series caused by temporal decorrelation [5, 6]. A loss-of-lock condition is created when no interferometric combination can be made between two coherent periods, resulting in a permanent loss of information during the incoherent period. An example is shown in Fig. 1, where loss-of-lock cuts the time series into four disconnected segments of coherent data. These can be visually identified by the block patterns created in the observed coherence matrix. Note that the intermittent loss of coherence in February of 2021 indicated by the cross pattern (contained within the third coherent segment from the left) does not constitute a loss-of-lock, because coherent interferometric combinations can be made across the decorrelated epoch.

These issues motivated the development of a new distributed scatterer (DS) InSAR processing methodology which is based on the integration of contextual data about the observed targets, documented in [5]. The key idea of this

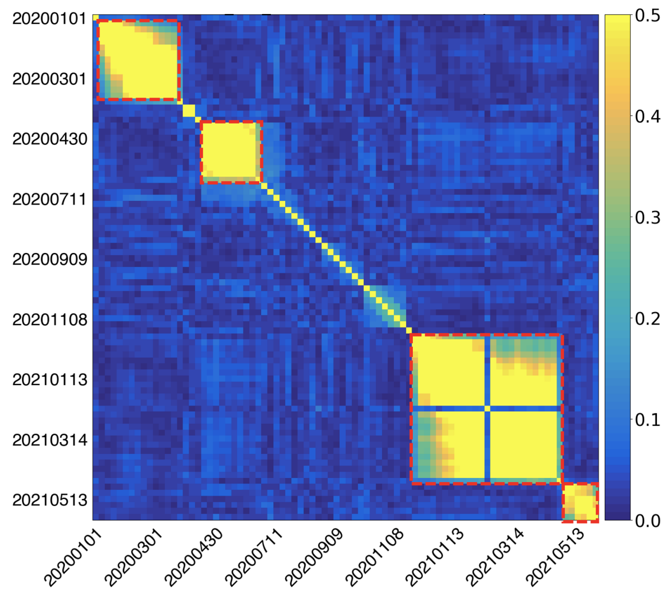

Fig. 1. Example coherence matrix of a multilooked agricultural parcel affected by loss-of-lock. Four disconnected coherent segments are outlined by the red dashed lines.

method is that additional information about the environment such as spatial land use, water management and soil data, along with temporal meteorological data is integrated into the processing framework to aid the algorithms in processing and interpreting the data. Thus breakages in the time series can be overcome by supplementing the incomplete SAR data stack with other knowledge of the region of interest.

Here we show the first application of this new methodology on a large scale which so far has only been tested on relatively small regions.

2. METHODOLOGY

2.1. DS Processing Method

The method used to process the data is detailed in [5], however, we introduce a new development that allows for the processing of time series data with different satellite revisit times. In previous iterations, the temporal phase unwrapping step required a constant revisit time, constraining our analysis to the period in which both Sentinel-1 A and B were operational. Section 2.2 describes the development of a new phase unwrapping method free from this constraint, allowing us to extend our analysis to times with only Sentinel-1 A coverage as well. For a full description of the method, the reader is directed to [5].

2.2. Temporal Phase Unwrapping

The presence of loss-of-lock results in a sparse time series of wrapped interferometric phases. The time series is sparse because it consists of segments (subsets) of coherent data, interspersed by incoherent periods. On their own, these sparse, wrapped phases cannot be interpreted due to the unknown displacement during the incoherent period and the highly nonlinear nature of the surface motion signal [5, 7]. Assuming that the true surface displacement can be described by a model, M, with unknown parameters, x, a basic representation of the mth coherent segment of the signal can be written as

$$W\Big\{\phi_m(t)\Big\} = W\Big\{\frac{-4\pi\cos\theta}{\lambda}\cdot\Big[M(x,t)+\Delta z_m\Big]+\epsilon\Big\}, \quad (1)$$

where ϕ is the interferometric phase, t is time, θ is the incidence angle, λ is the wavelength, Δz_m is a constant offset caused by the unknown vertical displacement which occurred during the incoherent period, ϵ is a combination of noise and model residuals, and $W\{\cdot\}$ is the wrapping operator. By taking the first order difference between the phases, we can omit any unknown constant in the time series caused by displacement during an incoherent period, resulting in the equation

$$W\Big\{\Delta\phi_m(t)\Big\} = W\Big\{\frac{-4\pi\cos\theta}{\lambda}\cdot\Delta M(x,t)+\epsilon_\Delta\Big\}, \quad (2)$$

where $\Delta\phi_m(t)$ is the differential form of $\phi_m(t)$.

Now the time series can be (implicitly) unwrapped by estimating the model parameters in x. This is done by minimizing the difference between the terms in the left and right sides of Eq. (2) in the complex domain. Treating these terms as the argument of a complex exponential function maps each wrapped phase to a point on the unit circle, and the error can be evaluated as the length of the vector between the points on the circle, giving the following cost function to be minimized:

$$\begin{aligned} C(\hat{x}) = \Big|\Big| &\exp\Big[i\cdot W\Big\{\Delta\phi_m(t)\Big\}\Big] \\ &- \exp\Big[i\cdot W\Big\{\frac{-4\pi\cos\theta}{\lambda}\cdot\Delta M(\hat{x},t)\Big\}\Big]\Big|\Big|, \end{aligned} \quad (3)$$

where i is the imaginary unit and C is the cost associated with the given set of estimated model parameters $\hat{x}$. Once the optimal set of model parameters is found, the time series segment can be unwrapped using the LAMBDA method [8].

In this representation, the model M can be any function parameterized by a set of unknown scalar values x. We use the "Simple Parameterization for the Motion of Soils (SPAMS)" model [9], which uses four scalar parameters to estimate shallow soft soil motion based on meteorological input data. For more detail on the definition and validation of this model, the reader is directed to [9].

This is where contextual information can significantly aid in the processing of the data; temporal data such as precipitation and evapotranspiration can be used to predict shallow ground motion, and the initial estimates of the model parameters can be obtained by studying the region's soil type and comparing to in-situ data, such as that in [10].

3. RESULTS AND DISCUSSION

3.1. Study Area

The area under study is known as the "Green Heart" (Dutch: *Groene Hart*) of the Netherlands, a primarily agricultural region encircled by the cities of Amsterdam, the Hague, Rotterdam and Utrecht. This region is represents a significant portion of the Dutch agricultural sector and comprises a large part of the subsiding Dutch coastal plain.

Some basic parameters of interest of the study area are shown in Table 1. Approximately nine years of Sentinel-1 data collected over four tracks are processed to provide subweekly time series estimates of surface motion on a parcel scale.

Table 1. Study Area Parameters

Parameter	Value
Sensor	Sentinel-1
Area	2165 km^2
Period	Jan. 2015 – Oct. 2023
Number of tracks	4
Number of images	1609
Number of parcels	31008

3.2. Time Series Result

An example of a parcel time series is shown in Fig. 2. This location is chosen because it is also a test site containing an in-situ measurement device, which allows for some validation of the obtained result. The four coloured traces in the plot are the resulting estimates of the four tracks used in the analysis. Gaps in the time series are the result of loss-of-lock, as discussed in Section 1. These gaps can be filled by combining observations of contextually similar parcels to create a spatial median as described in [5]. The overall root mean squared error of the four tracks when compared to in-situ data is 11.1 mm at validation site V1 (Zegveld, NL), and 8.8 mm at validation site V2 (Vlist, NL).

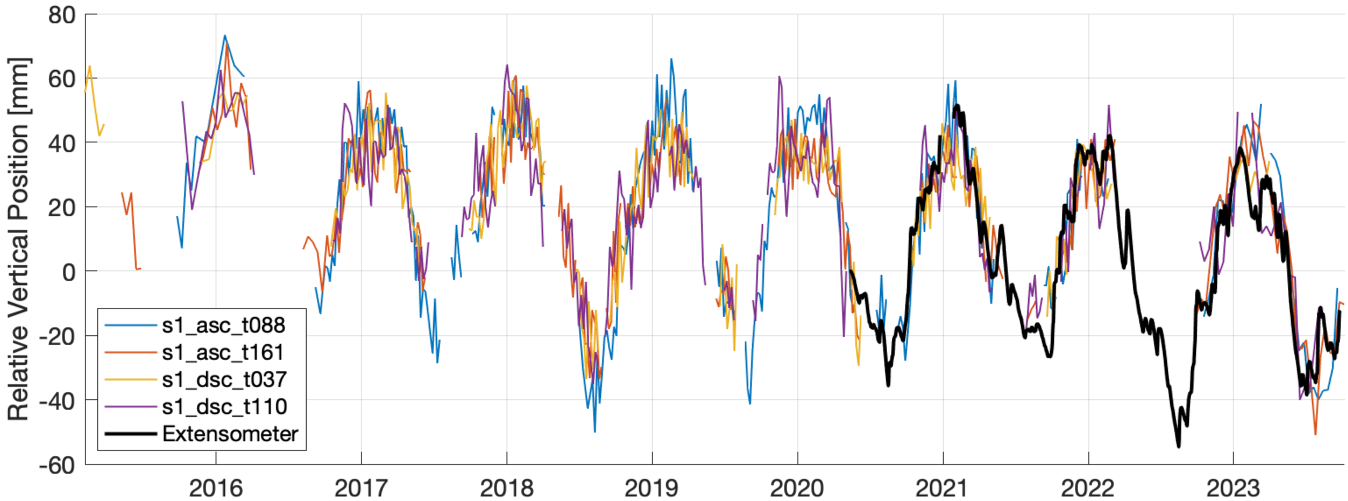

Fig. 2. Example time series result of a grassland parcel at validation site V1 in Zegveld, NL compared to in-situ data taken at that location. Blue, red, yellow, purple: estimated vertical soil displacement from Sentinel-1 tracks asc. 088, asc. 161, dsc. 037, and dsc. 110 respectively. Black: in-situ measurement.

3.3. Estimated Linear Subsidence Rates

A full time series has been estimated for each parcel, and linear subsidence rates can be derived by performing a simple linear regression on the result. This gives an average rate of irreversible subsidence for each parcel over the period of January 2015 to October 2023, which is shown in Fig. 3.

The overall mean subsidence rate of the region is 3.5 mm/year, and the greatest observed rate is 9.2 mm/year. The central region of the Green Heart near Gouda showed a larger rate of subsidence of approximately 5-10 mm/year, than the surrounding regions which ranged around 0-5 mm/year. This is in line with our expectations, as the region of Gouda experiences some of the most significant land subsidence of the municipalities located within the region.

In a related work [11], we show how measurements from other geodetic techniques such as levelling and airborne laser scanning can be integrated into a single dataset referenced to NAP, the Dutch vertical reference frame. Integrating the InSAR result into this dataset will allow for additional validation of the result.

4. CONCLUSION

We present the preliminary results of a wide-area InSAR study of the Dutch Green Heart region, the first of its kind which has been processed using a novel DS InSAR method designed for monitoring shallow soil motion. The estimated linear subsidence results show spatial correlation with the expected behaviour of the region, with the most significant soil loss occurring near the region of Gouda. The time series result is validated with the limited in-situ data available.

Additional work is still needed to validate the result, such as determining the accuracy of the estimated model parameters and the resulting model predictions, as well as comparisons with other geodetic measurements that have been performed in the region such as levelling and airborne laser scanning. Finally, we plan to integrate all the geodetic measurements into one consistent dataset in the Dutch vertical reference frame.

5. ACKNOWLEDGEMENT

This research is part of the Living on Soft Soils (LOSS): Subsidence and Society project, and is supported by the Dutch Research Council (NWO-NWA-ORC), grant no.: NWA.1160.18.259, URL: nwa-loss.nl.

6. REFERENCES

[1] Y. Morishita and R. F. Hanssen, "Temporal decorrelation in L-, C-, and X-band satellite radar interferometry for pasture on drained peat soils," *IEEE Transactions on Geoscience and Remote Sensing*, vol. 53, no. 2, pp. 1096–1104, 2015.

[2] Y. Morishita and R. F. Hanssen, "Deformation parameter estimation in low coherence areas using a multisatellite InSAR approach," *IEEE Transactions on Geoscience and Remote Sensing*, vol. 53, no. 8, pp. 4275–4283, 2015.

[3] L. Alshammari, D. J. Large, D. S. Boyd, A. Sowter, R. Anderson, R. Andersen, and S. Marsh, "Long-term peatland condition assessment via surface motion monitoring using the ISBAS DInSAR technique over the flow country, scotland," *Remote Sensing*, vol. 10, no. 7, 2018.

[4] T. Tampuu, F. de Zan, R. Shau, J. Praks, M. Kohv, and A. Kull, "Reliability of Sentinel-1 InSAR distributed scatterer (DS)

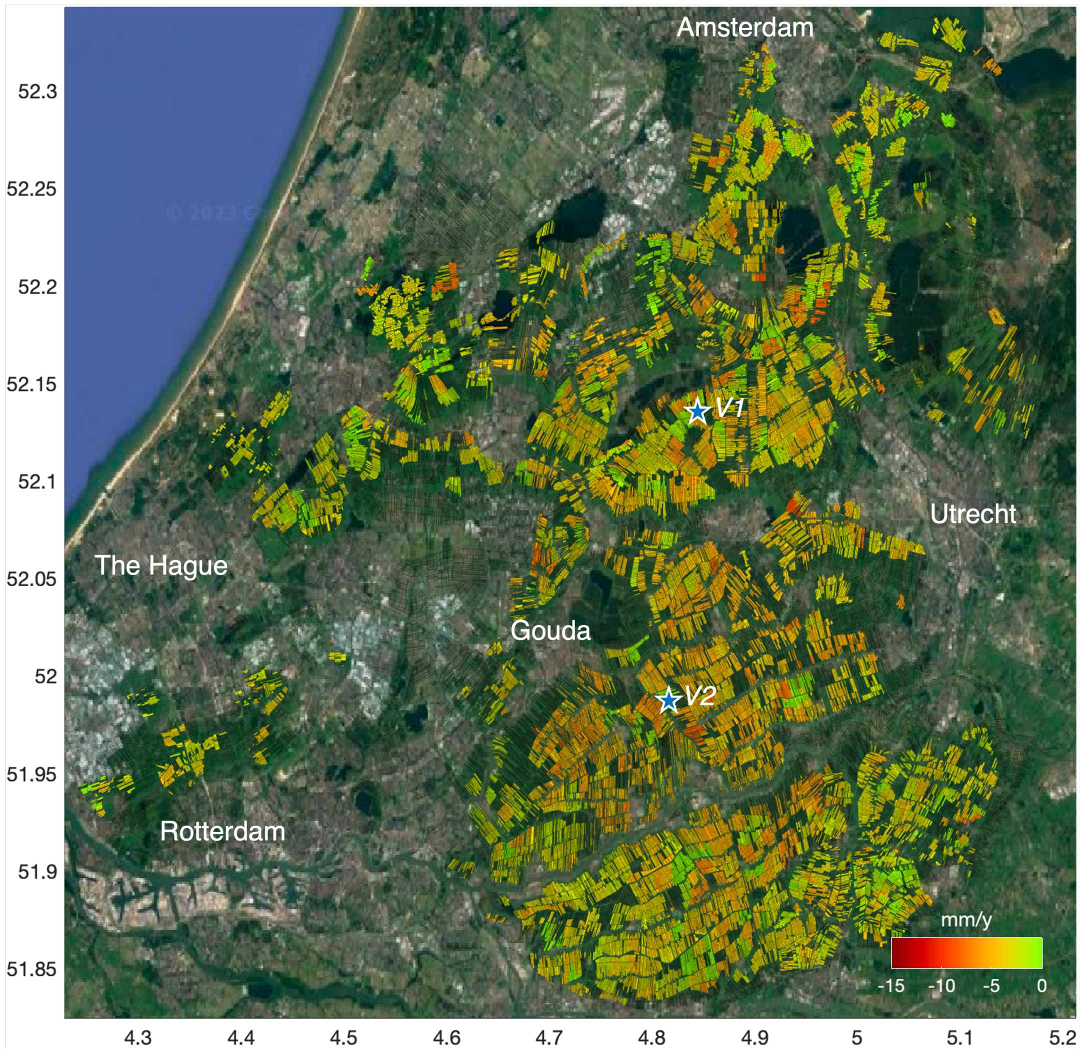

Fig. 3. Colour-coded map of estimated linear irreversible subsidence rates in the Green Heart region during the period Jan. 2015 – Oct. 2023. The stars mark locations of validation sites with in-situ data available.

time series to estimate the temporal vertical movement of ombrotrophic bog surface," in *EGU General Assembly*, Vienna, Austria, 2022, vol. EGU22-2387.

[5] P. Conroy, S. A. N. van Diepen, F. J. van Leijen, and R. F. Hanssen, "Bridging loss-of-lock in InSAR time series of distributed scatterers," *IEEE Transactions on Geoscience and Remote Sensing*, vol. 61, pp. 1–11, 2023.

[6] P. Conroy, S. A. N. van Diepen, F. J. van Leijen, and R. F. Hanssen, "Bridging InSAR coherence losses using contextual data driven processing," in *IGARSS 2023 - 2023 IEEE International Geoscience and Remote Sensing Symposium*, 2023, pp. 7864–7867.

[7] P. Conroy, S. A. N. Van Diepen, S. Van Asselen, G. Erkens, F. J. Van Leijen, and R. F. Hanssen, "Probabilistic estimation of InSAR displacement phase guided by contextual information and artificial intelligence," *IEEE Transactions on Geoscience and Remote Sensing*, vol. 60, pp. 1–11, 2022.

[8] B. Kampes and R. Hanssen, "Ambiguity resolution for permanent scatterer interferometry," *IEEE Transactions on Geoscience and Remote Sensing*, vol. 42, no. 11, pp. 2446–2453, 2004.

[9] P. Conroy, S. A. N. van Diepen, and R. F. Hanssen, "SPAMS: A new empirical model for soft soil surface displacement based on meteorological input data," *Geoderma*, vol. 440, no. 116699, 2023.

[10] S. van Asselen, G. Erkens, and F. de Graaf, "Monitoring shallow subsidence in cultivated peatlands," *Proceedings of the International Association of Hydrological Sciences*, vol. 382, pp. 189–194, 2020.

[11] S. van Diepen, P. Conroy, F. J. van Leijen, and R. F. Hanssen, "Towards a dynamic digital elevation model: a case study on the dutch peatlands," in *AGU Fall Meeting 2023*, San Francisco, United States, 2023.